

*Institute of Paper Science and Technology
Atlanta, Georgia*

IPST Technical Paper Series Number 958

**Stress Corrosion Cracking (SCC) and Corrosion
Fatigue Cracking (CFC) of a Duplex Stainless Steel in
White Water Environments**

**J. Perdomo, P. Singh, and J. Mahmood
J. Oteng**

December 2002

**Submitted to
Corrosion**

Copyright® 2002 by the Institute of Paper Science and Technology

For Members Only

INSTITUTE OF PAPER SCIENCE AND TECHNOLOGY PURPOSE AND MISSIONS

The Institute of Paper Science and Technology is an independent graduate school, research organization, and information center for science and technology mainly concerned with manufacture and uses of pulp, paper, paperboard, and other forest products and byproducts. Established in 1929 as The Institute of Paper Chemistry, the Institute provides research and information services to the wood, fiber, and allied industries in a unique partnership between education and business. The Institute is supported by 41 member companies. The purpose of the Institute is fulfilled through four missions, which are:

- to provide a multidisciplinary graduate education to students who advance the science and technology of the industry and who rise into leadership positions within the industry;
- to conduct and foster research that creates knowledge to satisfy the technological needs of the industry;
- to provide the information, expertise, and interactive learning that enable customers to improve job knowledge and business performance;
- to aggressively seek out technological opportunities and facilitate the transfer and implementation of those technologies in collaboration with industry partners.

ACCREDITATION

The Institute of Paper Science and Technology is accredited by the Commission on Colleges of the Southern Association of Colleges and Schools (1866 Southern Lane, Decatur, Georgia 30033-4097; Telephone number 404-679-4501) to award the master of science and doctor of philosophy degrees.

NOTICE AND DISCLAIMER

The Institute of Paper Science and Technology (IPST) has provided a high standard of professional service and has put forth its best efforts within the time and funds available for this project. The information and conclusions are advisory and are intended only for internal use by any company who may receive this report. Each company must decide for itself the best approach to solving any problems it may have and how, or whether, this reported information should be considered in its approach.

IPST does not recommend particular products, procedures, materials, or service. These are included only in the interest of completeness within a laboratory context and budgetary constraint. Actual products, materials, and services used may differ and are peculiar to the operations of each company.

In no event shall IPST or its employees and agents have any obligation or liability for damages including, but not limited to, consequential damages arising out of or in connection with any company's use of or inability to use the reported information. IPST provides no warranty or guaranty of results.

The Institute of Paper Science and Technology assures equal opportunity to all qualified persons without regard to race, color, religion, sex, national origin, age, disability, marital status, or Vietnam era veterans status in the admission to, participation in, treatment of, or employment in the programs and activities which the Institute operates.

STRESS CORROSION CRACKING (SCC) AND CORROSION FATIGUE CRACKING (CFC) OF A DUPLEX STAINLESS STEEL IN WHITE WATER ENVIRONMENTS

J.J. Perdomo, P.M. Singh, J. Mahmood
Corrosion and Materials Engineering Group
Institute of Paper Science and Technology, Atlanta, GA 30318-5794

J.E. Oteng
Nuclear and Radiological Engineering Program
Morehouse College and the Georgia Institute of Technology, Atlanta, GA 30314-3773

ABSTRACT

The present article addresses the stress corrosion cracking (SCC) and subsequent corrosion fatigue cracking (CFC) behavior of a heat-treated duplex stainless steel (DSS) in paper-machine white waters containing chloride and thiosulfate ions. According to the potentiodynamic and slow strain rate tests (SSRT) carried out in this study, it is believed that crack initiation corresponds to an SCC film rupture process during paper-machine shutdowns where ionic concentrations of species increase due to white water evaporation. Crack initiation occurs by pitting within ferrite grains or near grain boundaries where metallurgical changes produced during heat treatments play an important role. Once cracks have initiated, they will propagate by fatigue during alternate cycling loads produced in normal operation of the paper machine.

KEY WORDS: Duplex Stainless Steel, Heat Treatment, Stress Corrosion Cracking, Corrosion Fatigue, White Waters, Chloride, Thiosulfate.

INTRODUCTION

Suction rolls are used to remove water from paper at the wet end of the paper machine. One way to accomplish this is by passing the paper web through a roll nip, one roll of which is called the suction roll (Figure 1¹). The suction roll is typically drilled to an area of 20% and a

vacuum is applied to the inside to remove water¹. The critical component in the suction roll configuration is the drilled shell, which is subject to corrosion fatigue.

Duplex stainless steels (DSS) have replaced traditional suction roll materials due to their mechanical properties, superior corrosion resistance, and stress corrosion resistance. Duplex stainless steels are useful in highly oxidizing environments, chloride environments, and those containing H₂S. They have therefore earned a place in chemical plants, in the pulp and paper industry, in the oil and gas industry, in marine environments, and in heat exchangers². Today's suction roll materials for wet-end paper-machine processes are typically centrifugally cast precipitation hardening duplex stainless steel (DSS) alloys with roughly equal amounts of ferrite and austenite. Though cracking of suction rolls had been chronic for the paper industry in past decades with older metallurgies^{1,3-8} (e.g., bronze, martensitic and austenitic stainless steels, aluminum bronze, etc.), the use of DSS seems to have stopped the trend of failures originating by corrosion fatigue. However, the extent of the problem has not been well documented. Only a few studies report failures in suction rolls in certain types⁶⁻⁸, the most frequent being bronze and martensitic stainless steels which are no longer in use.

The characteristics of failure vary from roll to roll, but circumferential cracking in the middle of the roll predominates. Cracking may begin at the inside or outside surface of the roll shell, but cracking at the inside surface is apparently more common⁸. Figure 2 shows how cracks grow from inside the suction roll holes. Nearly all cracking is confined to the middle two thirds of the shell, where the largest bending moments are experienced. In terms of the environment, there have been few studies that correlate suction roll fatigue failure with metallurgy/fabrication and white water characteristics⁸⁻¹⁰.

Suction rolls are subjected to a variety of corrosive environments. The severity of the environment depends primarily on the type of paper produced and the degree of closure (volume of water used per ton of paper produced). Bacterial corrosion can occur, especially in creviced areas, such as suction roll holes filled with pulp, where biocides cannot reach. The corrosivity of white water depends primarily on the pH, temperature, and the concentrations of aggressive inorganic anions, such as chloride and thiosulfate. Chloride concentration increases with closure and causes pitting of the metal¹. Sulfate ions, however, are not considered aggressive, and they are thought to shield the effect of pitting when found in larger molar concentrations than chloride. Nonetheless, sulfate increases conductivity of the solution and hence environment corrosivity¹¹⁻¹³. Additionally, if sulfate-reducing bacteria are present, sulfate will indirectly promote localized corrosion¹⁴. Another critical anion in the pitting process is thiosulfate ion. Thiosulfate ions arise from hydrosulfite solutions used for brightening. The warm decomposition from those solutions will increase the amount of thiosulfate due to the slow kinetics of oxidation to form more stable sulfate. According to Bowers¹⁴, the worst case of thiosulfate pitting is said to occur in the molar concentration ratio range of sulfate and chloride to thiosulfate from 10 to 20. Above the range presented by the ratio, there is insufficient thiosulfate to reach the pit nucleus. Below this range, there is too much thiosulfate reduction to bisulfate, which would prevent the acidification of the pit required for further growth. Although duplex stainless steel suction roll materials have not been reported in the public literature as susceptible to corrosion fatigue in the early work published^{1,3-8} and in a recent exploratory work conducted in simulated paper-machine water⁹, there are some recent indications that pitting may act as initiation sites for stress corrosion cracking (SCC) in DSS¹⁵⁻¹⁶. For instance, two cast suction press rolls with the following compositions: C-0.06, Si-0.5, Mn-0.8, Cr-26, Ni-6.8 in wt% (similar to UNS J93423)¹⁵; and C-0.06, Si-0.8, Mn-0.6, P-0.030, S-0.006, Cr-20.0, Ni-5.0, Mo-2.0, Cu-4.5 in wt% and some nitrogen (similar to UNS J93372)¹⁶, have been reported to fail presumably by a stress corrosion cracking (SCC) mechanism initiated at pits in the form of IGC caused by increased ionic concentration of either thiosulfate or chlorine ions, respectively,

followed by a corrosion fatigue cracking (CFC) mechanism. Both cases pointed to carryover problems that increased the thiosulfate and chloride concentrations in each case.

Previous work on this area¹⁷ attempted to show the susceptibility of a heat-treated DSS to corrosion fatigue cracking in actual white waters with increased chloride concentration. Under the environmental conditions tested (up to 2000 ppm of chloride ions) the authors observed that the cracking behavior was more closely related to the metallurgical phases produced by heat treatments than it was to the white water composition. Nevertheless, it is also believed that ionic concentrations will increase greatly as a consequence of water evaporation during the frequent shutdowns experienced in paper machines¹⁶. This is in fact a key issue since the critical pitting temperature (CPT) in chloride environments for DSS decreases dramatically with chloride concentration¹⁸. The present study is aimed at furthering our current understanding of the stress corrosion-related initiation mechanism and consequent corrosion fatigue that produces failures of a commonly used DSS cast suction roll material in actual white waters with increased chloride and thiosulfate concentrations that represent process upsets in the paper machine.

EXPERIMENTAL TECHNIQUE

The specimens used to assess susceptibility of the duplex stainless steel used in this study were machined from centrifugally cast DSS roll material (C-0.06, Si-0.92, Mn-0.76, P-0.030, S-0.006, Cr-19.15, Ni-5.23, Mo-2.01, Cu-3.70 in wt% similar to UNS J93372). Since suction roll cast duplex alloys are usually heat treated to avoid second-phase particles, four different heat treatments were given to the specimens to obtain different microstructures, namely HT1, HT2, HT3, and HT4 (Table 1). Though no information was available for the time temperature transformation (TTT) diagram for the DSS used, an attempt to form different phases was made according to some early work published in UNS S32404-type material¹⁹⁻²⁴. According to this approach, and assuming a similar behavior, $M_{23}C_6$ compounds or even σ -phase are expected to form with HT1, whereas alpha prime (α') is expected to form with HT4. Alpha prime (α') phase is a chromium-rich base form of alpha, i.e., with the same crystalline structure, which is known to cause embrittlement¹⁹⁻²⁴. HT3 and HT2 will provide purely austenite (γ) and ferrite phases (α) with and without stress relief, respectively. Heat-treated specimens were metallographically prepared and observed under the optical microscope. All tests were done in the white water environments listed in Table 2. When appropriate, thiosulfate was added to match the worst case for chloride/thiosulfate pitting (the worst case is said to occur in the molar concentration ratio range of sulfate and chloride to thiosulfate from 10 to 20)¹⁴. All SSRT's were conducted at 50°C.

Two types of tests were carried out. The first type was standard potentiodynamic polarization measurements carried out according to ASTM G 5²⁵. They were performed to characterize passivity of the different heat-treated DSS in different environments. Rectangular samples with an area of roughly 4 cm² were polished to 1000-grit paper, rinsed, and degreased with double distilled water and acetone prior to testing. The selected scan rate was 0.5 mV/s starting at potentials cathodic to the open circuit potential. Potentials were measured with respect to a standard calomel electrode (SCE). Current densities in this study are reported in A/cm². The second type of measurements was slow strain rate tests (SSRT) using tensile specimens as described elsewhere²⁶. SSRT were conducted to determine the susceptibility of heat-treated samples to SCC in relevant environments. Samples were 3.875 inch (10 cm) long, 0.250 inch (6 mm) diameter. The useful gauge of the specimens was 1 inch (2.54 cm) long and had a 0.125 in (3 mm) diameter. The SSRT were conducted at 2×10^{-6} s⁻¹.

RESULTS AND DISCUSSION

Heat Treatment of DSS's

Figure 3 shows the microstructure obtained for the four heat treatments performed on the DSS. Samples have been etched with Vilella's reagent²⁷. This etchant is good for ferrite-carbide structures and produces grain boundary contrast of austenite. As depicted in Figures 3(a) and 3(d), these are the only heat treatments that provided some kind of microstructural change resolved by optical microscopy. HT2 and HT3 micrographs produce no visible precipitation. It is possible that $M_{23}C_6$ compounds are present in HT1 as fine precipitates observed along grain boundaries and within ferrite phase (α). Also, alpha prime (α') phase may be expected for heat treatment HT4; however, it is not usually resolved by optical microscopy¹⁹⁻²⁰. It isn't certain whether α' had formed or not, but some carbide precipitates were revealed by the reagent especially where thickening of the grain boundaries was observed. Further work is required to appropriately identify the nature of the phases formed.

Potentiodynamic Behavior

Figure 4 shows the electrochemical behavior of each heat treatment (Table 1) as a function of each individual white water composition shown in Table 2. For the case of WW1 (200 ppm of Cl⁻) shown in Figure 4(a), there seems to be clear evidence of the passivation of the metal as a function of heat treatment. In general, HT3 shows the best passivation behavior, with a relatively large passivation potential range and the smallest passivation current density shown. Passivation currents for the rest of the heat treatments in WW1 relative to each other are as follows: HT3<HT2<HT4~HT1. Similar trends for all heat treatments were obtained for WW2 and WW3, where chloride concentrations have been augmented in ten-fold increments and thiosulfate kept to a minimum (Figures 4(b) and 4(c), respectively). However, the potential range for passivation seems to narrow with chloride content in WW2 and WW3. In the case of WW3, the range is limited to -100 to +100 mV-SCE in all heat treatments. It also seems that the passivation potential range is more dependent (linear) on current for WW2 and WW3 in contrast with the results obtained for WW1 (Figure 4(a)).

The addition of thiosulfate in the amounts shown in Table 2 makes the anodic behavior more complex to interpret. As shown in Figure 4(d) for WW4, HT3 exhibits the best passivation behavior; however, the passivity regions are less defined than those obtained for white waters without thiosulfate (WW1, WW2, and WW3). In the cases of HT2, HT3, and HT4, a "nose" is evident at around +0.300 V-SCE. The nose indicates the onset of passivation but there is a marked dependence of the passivity region on current density. So in the same environment, different heat treatments passivate at different potentials when thiosulfate ions are added. This may also be due to the oxidation of thiosulfate to sulfate ion. In the case of WW5 (Figure 4(e)) and WW6 (Figure 4(f)), HT3 and HT2 show more defined passivation regions, whereas HT1 and HT4 do not. Consistently, HT1 and HT4 show the worst performance as far as passivation is concerned under the tested environments.

From the potentiodynamic test results obtained here, it is not clear that thiosulfate additions at the specified ratios shown in Table 2 worsen pitting behavior of the heat-treated duplex stainless steels as reported earlier¹⁴. As shown, HT1 in WW1, WW5, and WW6 exhibit the best passive regions whereas in WW2, WW3, and WW4 almost no passivation is shown. In the case of HT2, passivation is obtained in WW1, WW4 (in this particular case at more positive potentials than the rest of white waters), and WW6. HT3 shows passivation in almost all cases

other than WW3. In the case of HT4, passivation is attained in WW1, WW4, WW3, and WW6. Again, regions of passivity, potential ranges, and passivation currents vary in each case.

Slow Strain Rate Tests (SSRT)

SSRT were performed on a number of heat treatments and environments. As far as heat treatments are concerned, HT1 and HT4 were selected due to the relatively poor passivation performance based upon the potentiodynamic tests, whereas HT3 was selected for its relatively good passivation behavior. In the case of environments, WW3 and WW6 were chosen due to the large concentration of chloride present. Figures 5(a) to 5(c) show the results of SSRT for HT1, HT3, and HT4 in both WW3 and WW6 environments, respectively. As it can be depicted in Figure 5(a), HT1 seemed to be unaffected by the environment, since both curves are well within the experimental error. No loss of ductility or any other measurable property change was reported in terms of percentage of elongation, area reduction, or hardness (Table 3). So it seems that the expected formation of chromium carbides did not compromise the performance of the DSS under the tested conditions.

In the case of HT3 (Figure 5(b)), there seems to be an effect of the environment, since the times to failure varied. Also, differences in area reduction and elongation are smaller by 17% and 6%, respectively, in WW3 than they are in WW6 (Table 3). However, no physical evidence of cracking was observed upon inspection of the surface of the tensile sample gauge. HT4 (Figure 5(c)), though, shows the most significant difference between WW3 and WW6 as far as time of failure is concerned (~10% strain difference). The percentage of elongation difference was 9%, whereas area reduction was ~ 50% difference between WW3 and WW6 (Table 3). It can also be seen that the performance of the alloy with HT4 in WW6 and air are very similar (Table 3 and Figure 5(c)). Evidence of cracking along the gauge for HT4 in WW3 was physically observed as shown in Figure 6(a). The fracture surface (Figure 6(b)) shows a mixed brittle-ductile fracture mode. The brittle portion of the sample is located near the gauge surface (Figure 6(c)) as evidenced by the observed river marks that describe the direction for crack propagation in typical transcrystalline fracture. Ductile areas are visible close to the center of the sample where a microvoid coalescence mechanism is shown by the formation of dimples by either precipitate cracking or interface failure with the matrix (Figure 6(d)). The void diameter size and separation of the dimples are related to the precipitate dimensions.

The morphology of the cracks along the tensile specimen gauge (Figures 7(a) and 7(b)) suggests that initiation occurred earlier during the test, and they stopped growing in depth and yielded with further straining. Typical initiation cracks start either within the ferrite phase (dark) or near the ferrite/austenite grain boundary and proceed until they are arrested by austenite (light phase) (Figures 7(a) and 7(b)). At least, this seems to be the initial stage of failure. Curiously, no secondary cracking (branching out) was observed. Crack growth rates were estimated by sectioning the tensile specimen gauge and by measuring the longest crack observed away from the necked area during the entire duration of the test. The deepest crack measured by sectioning the sample was of roughly ~20 μm providing a crack growth rate of 16 $\mu\text{m}/\text{d}$. However, cracks as deep as 50 μm were observed on the surface using the SEM. In essence, the large (2%) chloride concentration, in combination with the microstructural changes produced in HT4, seem to enhance pitting in areas where ferrite chemical composition has been affected by heat treatments (presumably α' phase) causing selective corrosion of such areas. This serves as the initiation site for stress corrosion cracking. This is certainly consistent with claims of chloride-SCC of similar stainless steels by a film rupture mechanism²⁸⁻²⁹. However, the presence of thiosulfate for HT4 in WW6 seems to inhibit pitting. It is likely that thiosulfate may have been oxidized to sulfate which is the thermodynamically

stable form of sulfur in white waters. Sulfate is known to be a non-aggressive ion; in fact, it acts as an inhibitor for chloride pitting¹. Either ferrite pitting or well-initiated transgranular cracks can play a significant role in the suction roll fatigue life once they have started by SCC. They can continue to grow via either corrosion fatigue cracking mechanism (CFC) or by pure fatigue loading to produce multiple cracks on the surface as described in an earlier study¹⁷. These multiple cracks may in turn interact and coalesce with each other causing the failure of suction rolls. A continuing transgranular crack growth (TGC) is expected under these conditions.

CONCLUSIONS

According to the potentiodynamic study performed on different heat treatments, chloride concentration increase of itself has a significant effect on the anodic behavior of all heat treatments tested, worsening passivation properties.

It is not clear that thiosulfate additions at the specified ratios of this study enhance pitting behavior, as it has been reported earlier, at least for this heat-treated duplex stainless steel. Depending on the heat treatment and chloride concentration, thiosulfate may or may not enhance pitting.

Heat treatments such as HT3 seem to prevent environmentally assisted cracking problems under the conditions tested.

Pitting and subsequent cracking of HT4, in the largest (2%) chloride concentration tested here, occurs at either ferrite or near the ferrite/austenite grain boundaries. This suggests that the phase present in ferrite formed during HT4 may have been responsible for the poor performance observed in WW3.

Thiosulfate additions in this study did not favor pitting. In the case of SSRT's for HT4 in WW6, thiosulfate additions inhibited the aggressive effect observed for HT4 in WW3. It is believed that oxidation of thiosulfate to sulfate may have occurred. Sulfate is the most stable sulfur species in white waters, and it is known to have an inhibiting effect on chloride-related pitting.

Pitting on ferrite with HT4 in 2% chloride environments may act as initiation sites for SCC under stress following transcrystalline crack growth (TGC). Once cracks have reached a critical size, either CFC or pure fatigue loading may continue during normal operation of the rolls as described in an earlier study¹⁷ with a transgranular-cracking mode.

In the case of HT1, the presence of chromium carbides did not compromise the mechanical performance of the DSS under high chloride environments despite the poor passivation properties revealed during anodic polarization.

The formation of precipitates during heat treatments of the DSS used in this study requires further electron microscopy work to identify chemical composition and nature of the phases.

REFERENCES

1. D.A. Wensley, M.D. Moskal, "Paper Machine Suction Roll Corrosion", Metals Handbook, Vol 13, 9th Edition "Corrosion", p. 594, ASM International, Metals Park, OH (1987).
2. P. Lacombe, B. Baroux, G. Beranger, "Stainless Steels", Les Editions de Physique Les Ulis, France (1993).
3. C.B. Dahl, E.P. Neubauer, "Modern Practices Can Present Hazards to SS Suction Rolls", Paper Trade Journal, p. 46, August 23 (1971).
4. J.B. String, Modern Suction Roll Design and Construction, Proc. Technical Section, CPPA, p. D-74-D79 (1964).

5. R.M. Vadas, "The Suction Roll – Its problems and its future", *Pulp and Paper Canada*, 72(11): p. 66 (1971).
6. A. Garner, "Suction Roll Failure in Canada", Proc. 70th Annual Meeting of the Canadian Pulp and Paper Association, Montreal, p. 36 February (1984).
7. F. Wooster, M. Moskal, J. McNamee, *TAPPI Journal*, 62 (9), p. 71 (1979).
8. R.A. Yeske, "Fundamentals of Corrosion Control in Paper Mills", IPST Project No. 3309, Atlanta, GA, pp. 5-44, September 11 (1985).
9. G.J. Fonder, P.M. Singh, J. Mahmood, "Annual Program Review Corrosion Control", IPST Project No. F019, Atlanta, GA, p. 40, March 8 (2000).
10. R.A. Yeske, "Prediction of Suction Roll Performance from Laboratory Testing", *NACE Corrosion '86 Proceedings*, Paper No. 147 (1986).
11. D.A. Wensley, "Localized Corrosion of Stainless Steels in White Waters", *Materials Performance*, 28 (11), p. 68 (1989).
12. D.C. Bennet, C.J. Federowicz, "Prediction of Localized Corrosion of Stainless Steels in White Waters", *Material Performance*, 21 (4), p. 39 (1982).
13. R.C. Newman, "Pitting of Stainless Steel Alloys in Sulfate Solutions Containing Thiosulfate Ions", *Corrosion* 41 (8), p. 450 (1985).
14. D.F. Bowers, "Corrosion in closed white water systems", *TAPPI*, Vol. 61, No. 3, p. 57 (1978).
15. CC Technologies, Failure Analysis Examples in the Pulp and Paper Industry (<http://www.cctechnologies.com/services/pulpaper/index.htm>).
16. J.J. Perdomo, P.M. Singh, "Failure Analysis of Failed Suction Roll Material DSS KCR-A682", IPST Confidential Report, Atlanta, GA, June 2001.
17. J.J. Perdomo, P.M. Singh, "Corrosion Fatigue Behavior of a Heat Treated Duplex Stainless Steel in Paper Machine White Waters", *Corrosion Reviews*, Vol. 20, No. 4-5, pp. 295-316 (2002).
18. S. Bernhardson, "Duplex and High Nickel Stainless Steels for Refineries and the Petroleum Industry", *NACE Corrosion '85 Proceedings*, Paper No. 165 (1985).
19. H.D. Solomon, T.M. Devine, "Duplex Stainless Steels", *Conference Proceedings/American Society for Metals*, Edited by R.A. Lula, pp. 693-756 ASM (1983).
20. H.D. Solomon, T.M. Devine, *American Society for Testing and Materials*, Philadelphia, PA, ASTM STP 672, pp. 430-461 (1979).
21. P. Lacombe, B. Baroux, G. Beranger, "Stainless Steels", *Les Editions de Physique Les Ulis, France* (1993).
22. J.O Nilsson, "Materials Science and Technology", Vol. 8, August, pp. 685-700 (1992).
23. R.N. Gunn, "Duplex Stainless Steels, Microstructure, Properties and Applications", *Arlington Publishing, Cambridge, England*, (1997).
24. J. Charles, "Proceedings Conf. Duplex Stainless Steels", *Beaune, France, Les Editions de Physique*, Vol. 1, pp. 3-48 (1991).
25. ASTM G 5, "Standard Reference Method for Making Potentiostatic and Potentiodynamic Polarization Measurements", *ASTM Book of Standards*, West Conshohocken, PA, 03.01, 816 (2001).
26. R.N. Parkins, "Stress Corrosion Cracking-The Slow Strain Rate Technique", *American Society for Testing and Materials*, Philadelphia, PA, ASTM STP 665, p.5 (1979).
27. G. Vander Voort, "Metallography, Principles and Practice", *Mc Graw Hill, New York*, pp. 336, 632-647 (1984).
28. K. Tamaki, Tsujikawa, Y. Hisamatsu, *Advances in Localized Corrosion*, HACE, Houston, TX, p. 207 (1991).

29. R.C. Newman, "Corrosion Mechanisms, Theory and Practice", Edited by P. Marcus and J. Oudar, Marcel Dekker, New York, p. 331 (1995).

TABLE 1. HEAT TREATMENT USED FOR STRESS CORROSION CRACKING OF DSS'S.

Heat Treatment	Description
*HT1	Aging at 800°C for 8 h, furnace cooled to room temperature.
*HT2	Solution annealing at 1100°C for 8 h, water quenched.
*HT3	Solution annealing at 1100°C for 8 h, water quenched; stress relief annealing at 630°C x 45 m, air cooled; second stress relief annealing at 560°C x 45 m, air cooled.
*HT4	Aged at 500°C for 6 h, water quenched to room temperature.

*HT: Heat Treatment

TABLE 2. ENVIRONMENTAL CONDITIONS IN [mg/L].

	SO_4^{2-}	$S_2O_3^{2-}$	Mg^{2+}	Cl^-	Ca^{2+}	Na^+
Air	N/A	N/A	N/A	N/A	N/A	N/A
*WW1	2100	<10	12	200	820	175
*WW2	2100	<10	12	2000	820	1,750
*WW3	2100	<10	12	20000	820	17,500
*WW4	2100	155	12	200	820	485
*WW5	2100	275	12	2000	820	2,525
*WW6	2100	1,475	12	20000	820	22,925

*WW: White water

TABLE 3. SCC RESULTS OF HEAT-TREATED DUPLEX STAINLESS STEELS IN DIFFERENT ENVIRONMENTS.

HT	WW	T/[°C]	% E	% AR	SCC cracks	CGR/[μm/d]
HT1	WW3	50	21	24	No	0
HT1	WW6	50	22	20	No	0
HT3	WW3	50	22	37	No	0
HT3	WW6	50	28	54	No	0
HT4	Air	50	33	72	No	0
HT4	WW3	50	21	21	Yes	16
HT4	WW6	50	30	72	No	0

WW: White water

E: Elongation

AR: Area reduction

CGR: Crack growth rate

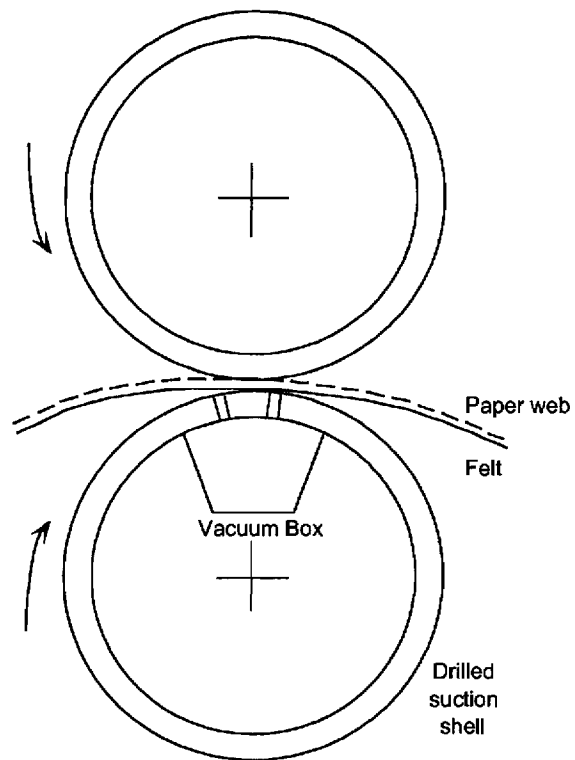


FIGURE. 1. Cross section of suction roll configuration¹.

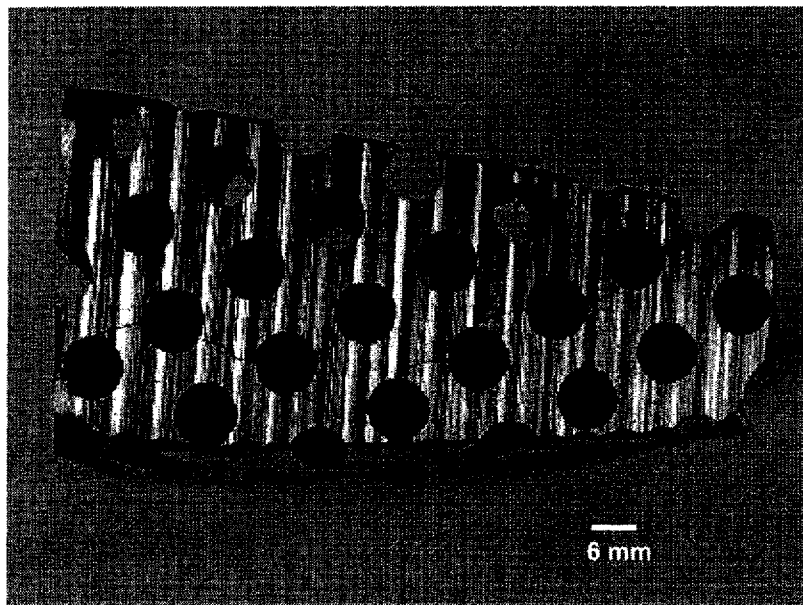


FIGURE 2. Suction roll sample of failed DSS (inside surface view)

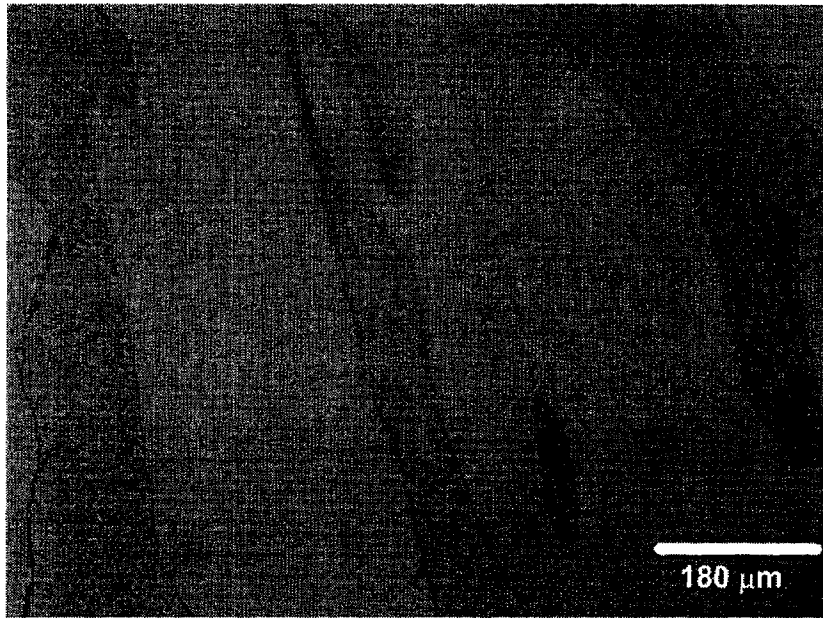


FIGURE 3(a). DSS microstructure after HT1, etched with Vilella's reagent for one minute

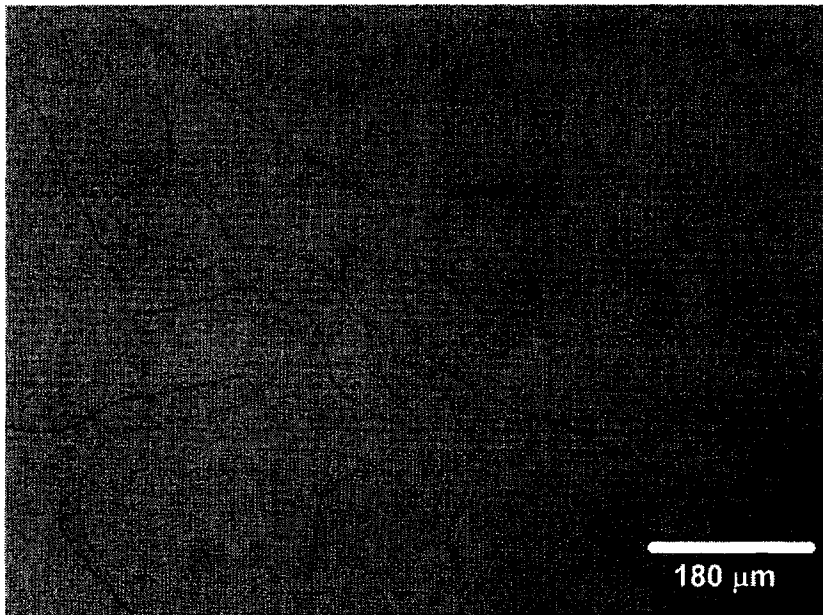


FIGURE 3(b). DSS microstructure after HT2, etched with Vilella's reagent for one minute.

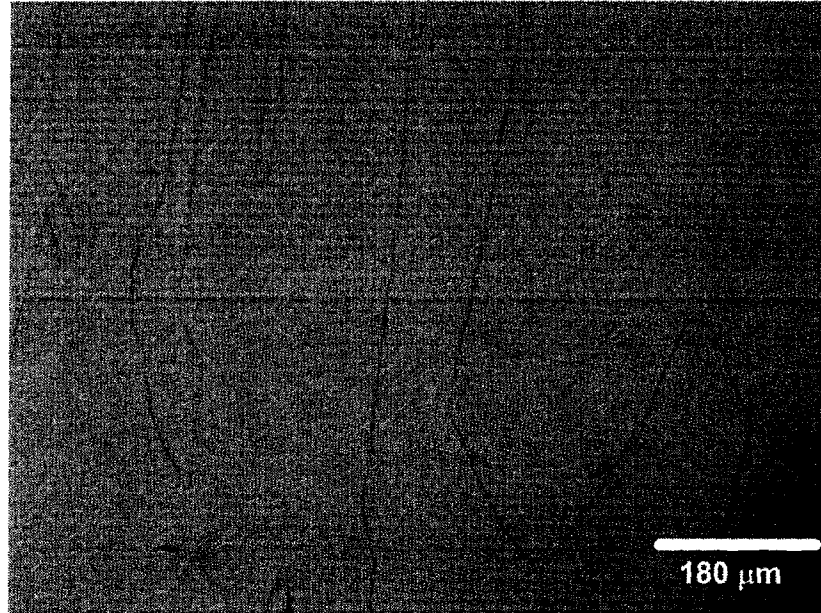


FIGURE 3(c). DSS microstructure after HT3, etched with Vilella's reagent for one minute

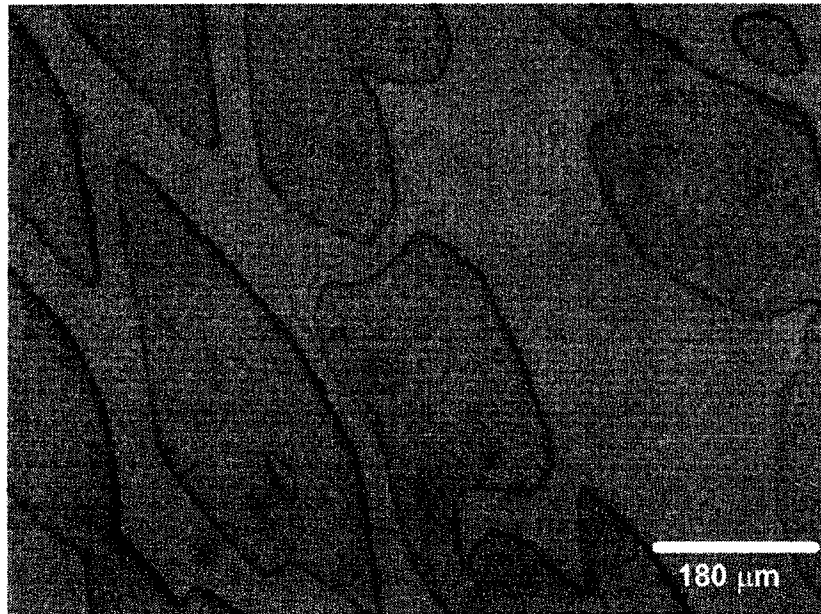


FIGURE 3(d). DSS microstructure after HT4, etched with Vilella's reagent for one minute.

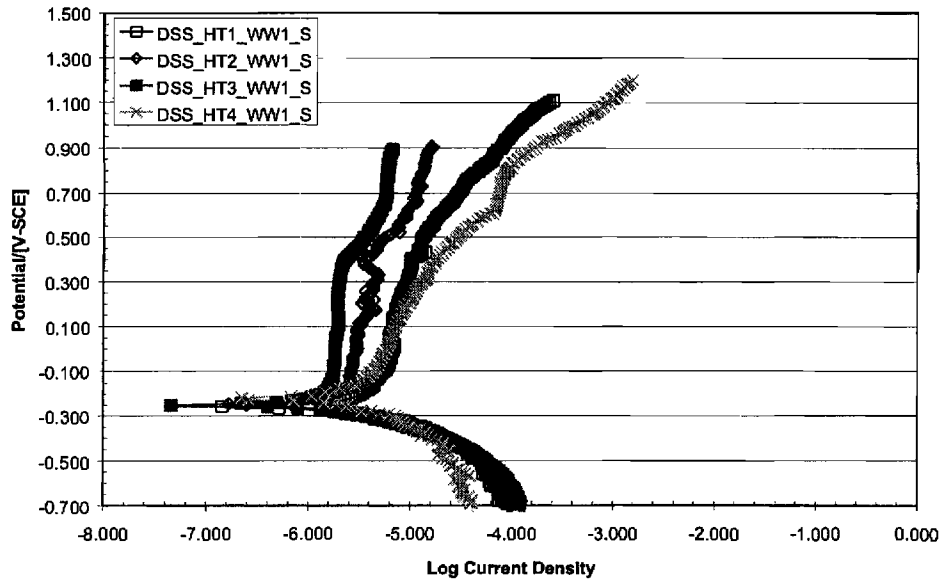


FIGURE 4(a). Potentiodynamic behavior of four different DSS heat treatments in WW1 at 50°C.

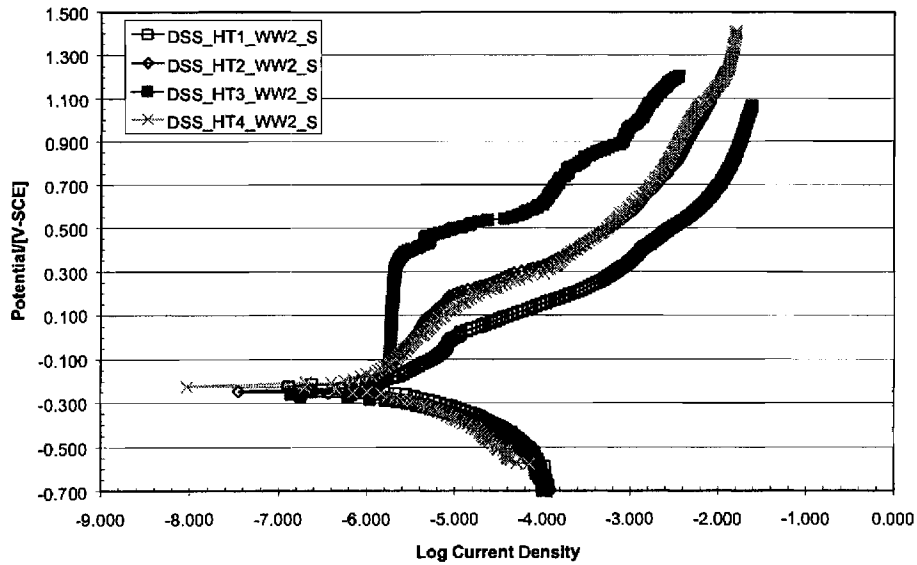


FIGURE 4(b). Potentiodynamic behavior of four different DSS heat treatments in WW2 at 50°C.

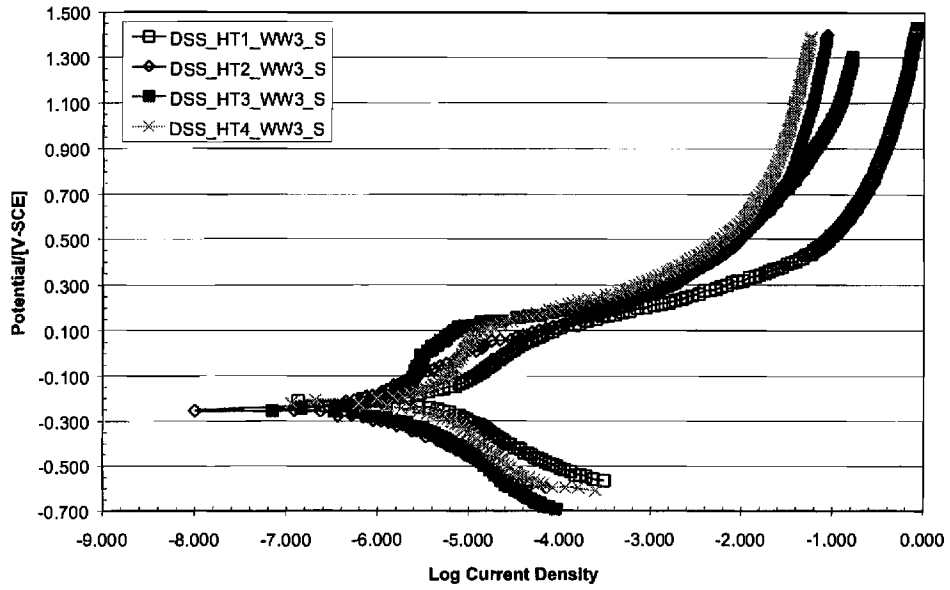


FIGURE 4(c). Potentiodynamic behavior of four different DSS heat treatments in WW3 at 50°C.

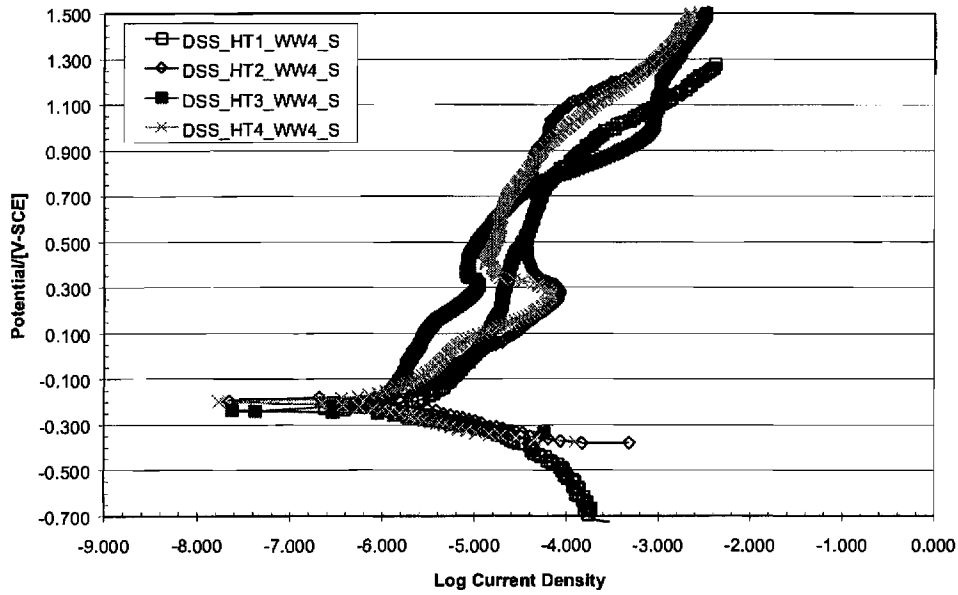


FIGURE 4(d). Potentiodynamic behavior of four different DSS heat treatments in WW4 at 50°C.

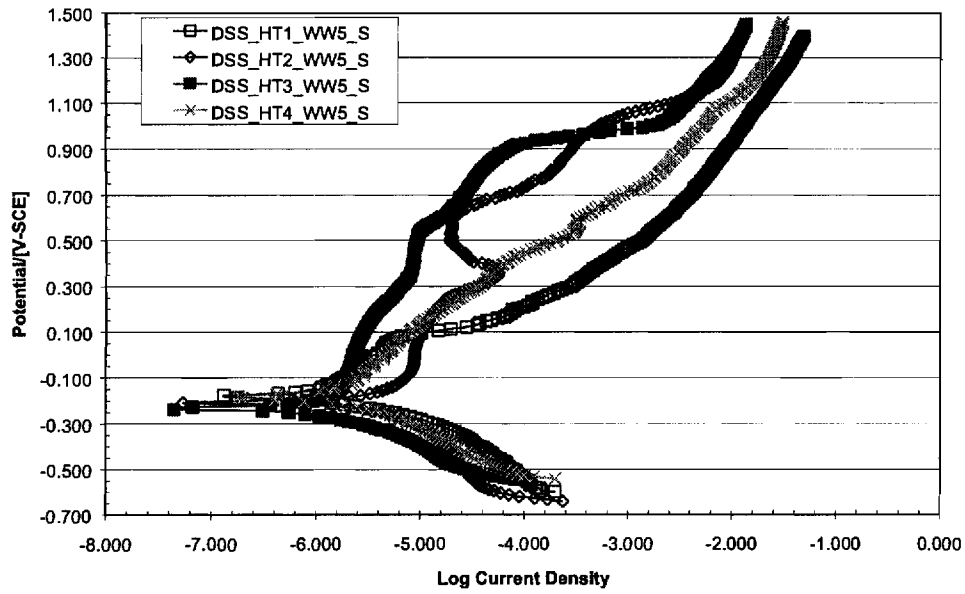


FIGURE 4(e). Potentiodynamic behavior of four different DSS heat treatments in WW5 at 50°C.

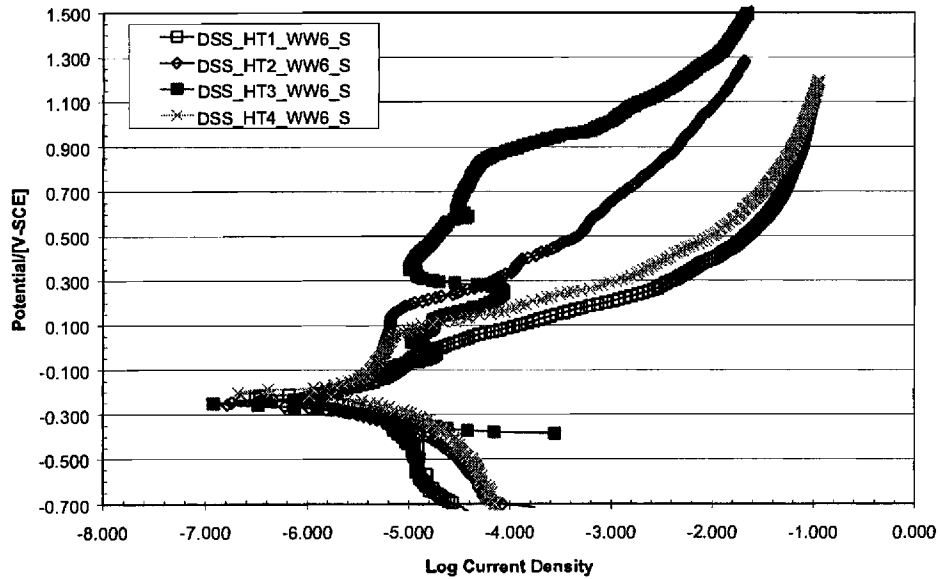


FIGURE 4(f). Potentiodynamic behavior of four different DSS heat treatments in WW6 at 50°C.

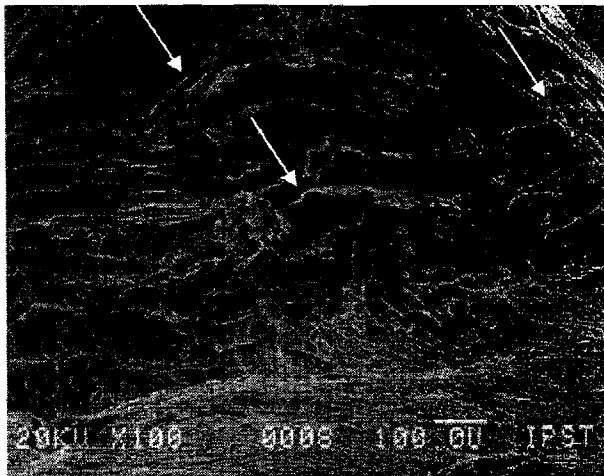


FIGURE 6(a). SEM micrograph showing surface cracks on DSS sample with HT4 in WW3.

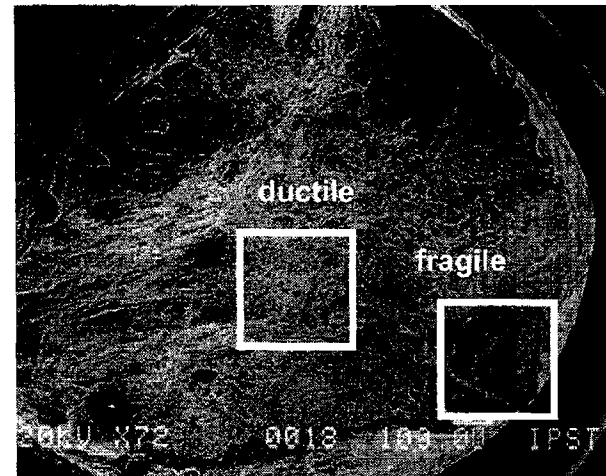


FIGURE 6(b). SEM micrograph showing fracture surface of DSS sample with HT4 in WW3.

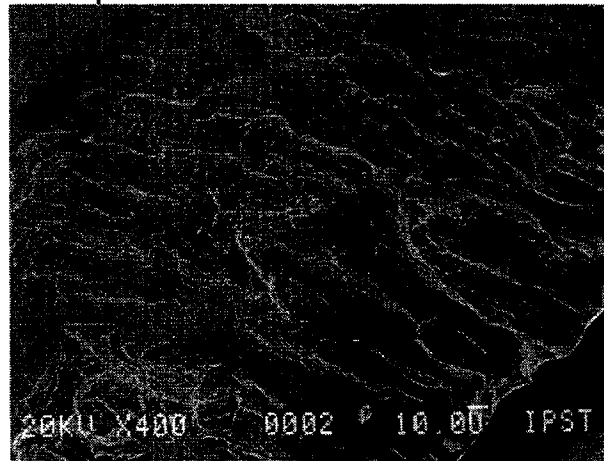


FIGURE 6(c). SEM micrograph showing brittle fracture region of DSS sample with HT4 in WW3.

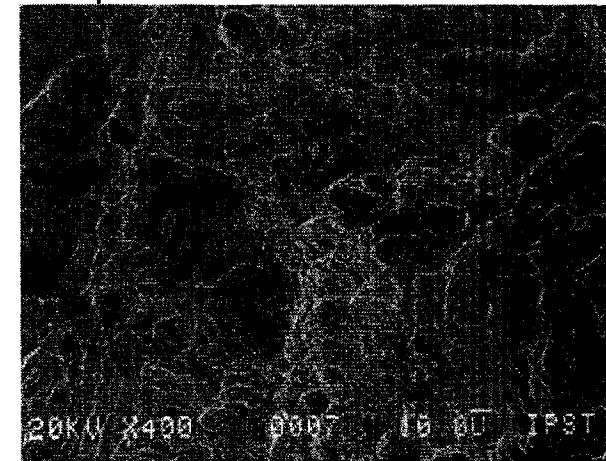


FIGURE 6(d). SEM micrograph showing ductile fracture region of DSS sample with HT4 in WW3.

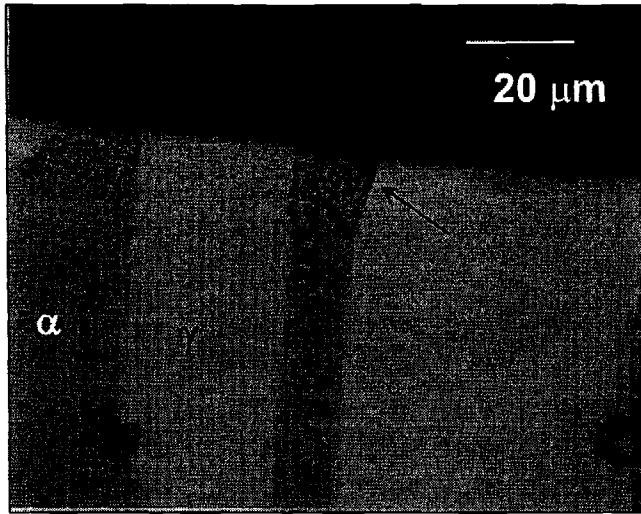


FIGURE 7(a). Stress corrosion crack on DSS in HT4 in WW3 revealed by using Kalling's reagent No. 2²⁷.

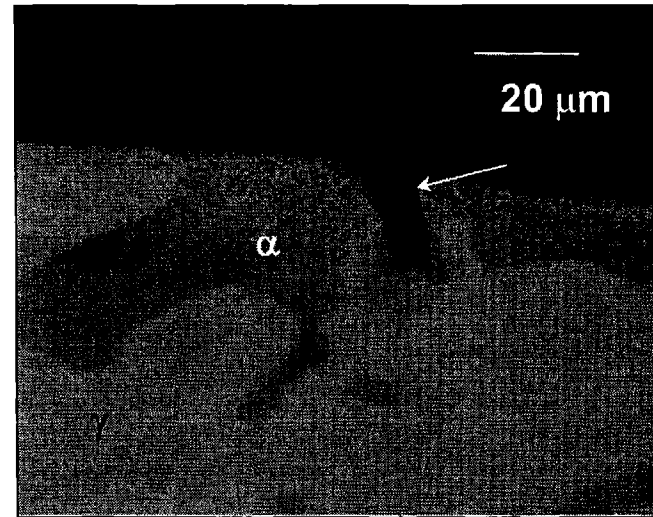


FIGURE 7(b). Pit on DSS in HT4 in WW3 revealed by using Kalling's reagent No. 2²⁷.